AISE/CORNELL UNIVERSITY
Crane Runway Girder Project

Document 86-1

June 23, 1986

Task IV

# FINAL REPORT

Volume 1 of 2

by

Prof. A. R. Ingraffea
Prof. W. McGuire
Prof. T. Pekoz
Dr. W. Gerstle
Mr. K. Mettam
Mr. P. Wawrzynek
Dr. A. K. Hellier

Table of Contents

List of Tables

List of Figures

## 1. Introduction

Crane runway girders are used to transfer the heavy wheel loads of traveling bridge cranes to the columns of mill buildings. A series of such girders, each used in a simple span configuration, comprises a runway for the crane, as in Figure 1. Although the primary stresses in crane runway girders are readily determined by plate girder theory, experience has shown that other, locally-induced stresses are important in the design of these girders against fatigue cracking.

This experience began in Europe in the late 1940's when mill buildings were reconstructed using three-plate welded girders in place of the former riveted design. A number of fatigue cracking problems began to arise in the very early part of the design life of these girders. Three such problems which are chronic and occurring in mills throughout the world are shown in Figure 2.

European literature on these and other cracking problems particular to welded girders began to appear in the early 1960's. These problems began to occur in mills in the United States in the same decade, and in some cases in epidemic proportions. In one mill a survey indicated at least 40% of runway girders with one or more of the types of cracking indicated in Figure 2. Although no loss-of-life failures have been reported, loss-of-service failures resulting from web buckling have occurred. Figure 3a shows a girder which has been removed from service. Cracks in the web-to-compression-flange weld, Type A in Figure 2, and in the stiffener-to-flange weld, Type C in Figure 2, can be seen in Figure 3b. Figure 3c shows a close-up of another web panel which has buckled due to loss of lateral restraint when the web-to-compression-flange weld cracked over the entire panel length. In addition to the cost of girder replacement is that due to

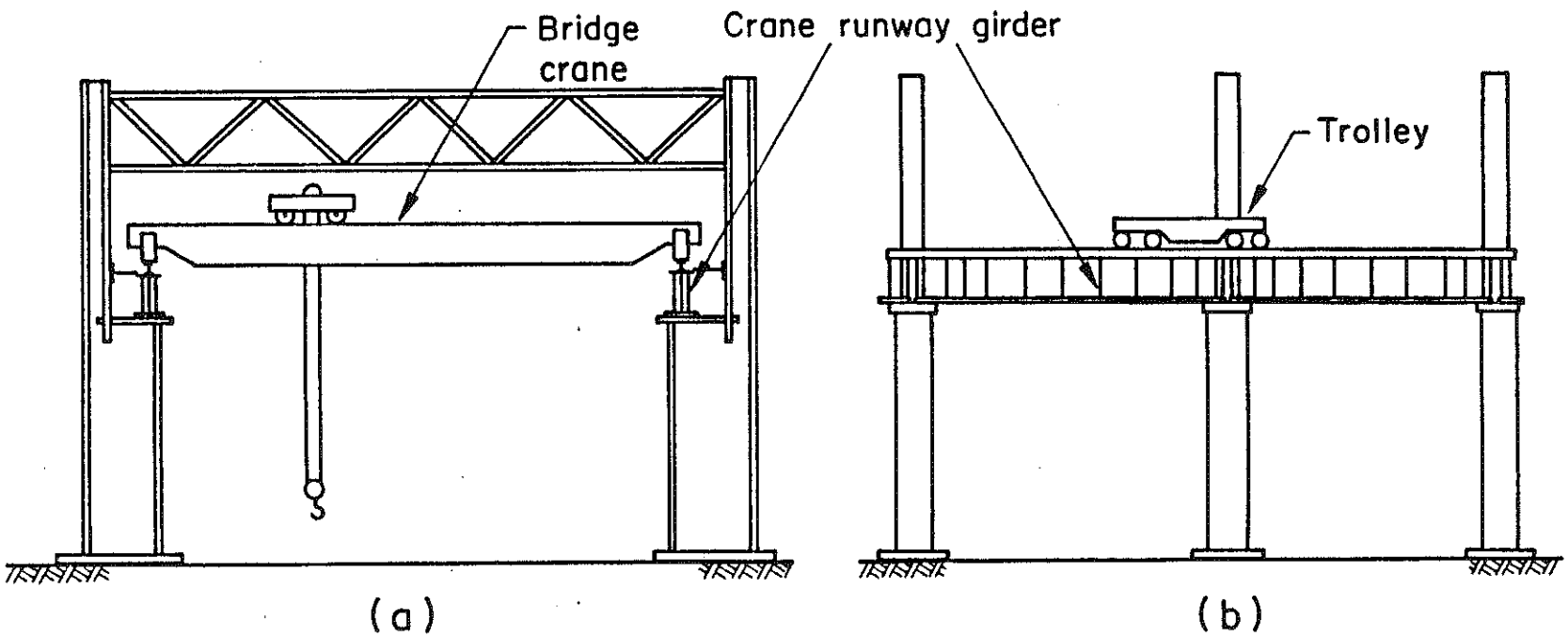


Fig. 1 Crane runway structure. a) End-on view of runway; b) Elevation of section of runway.

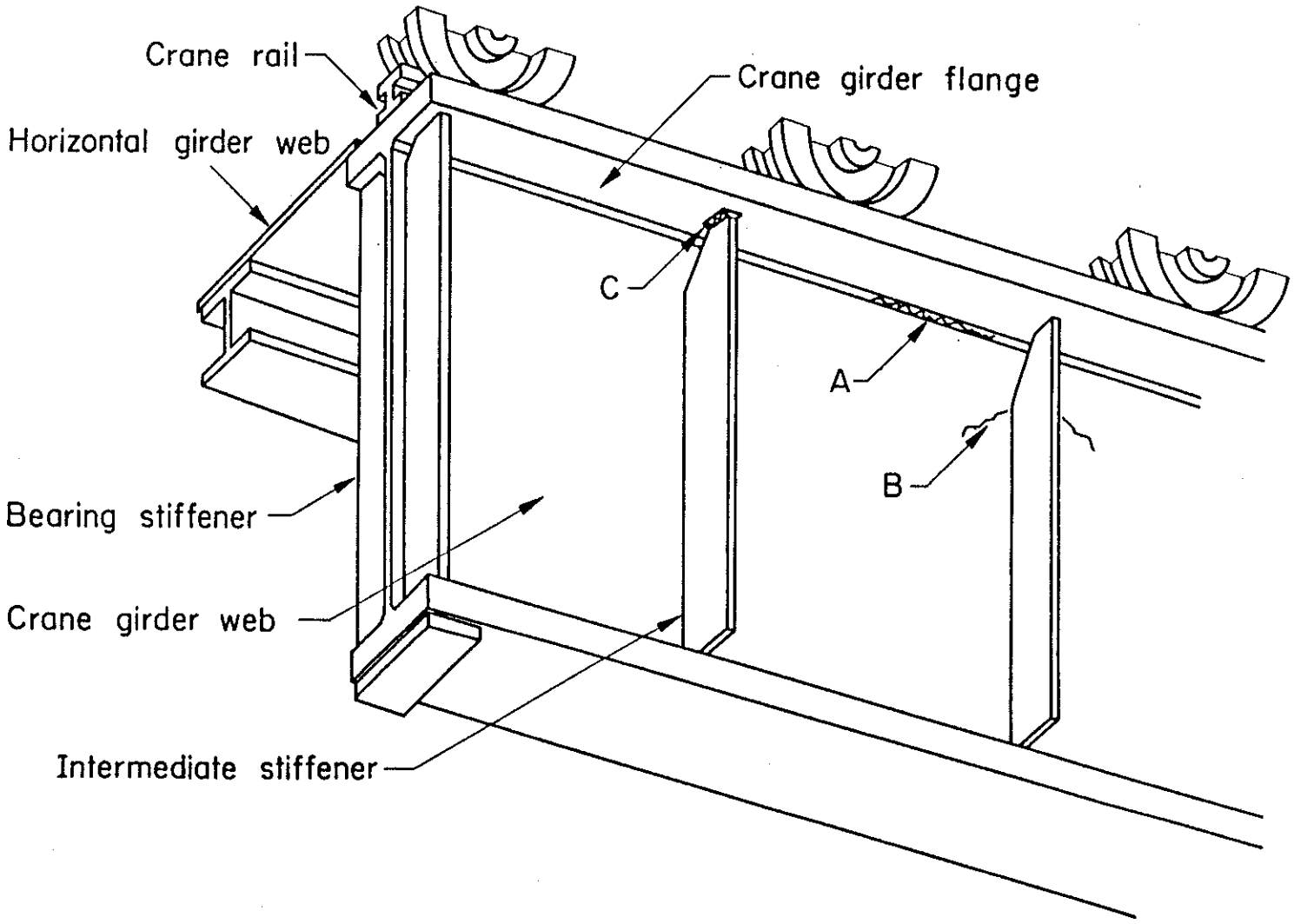


Fig. 2 Schematic of crane runway girder and observed cracking types.

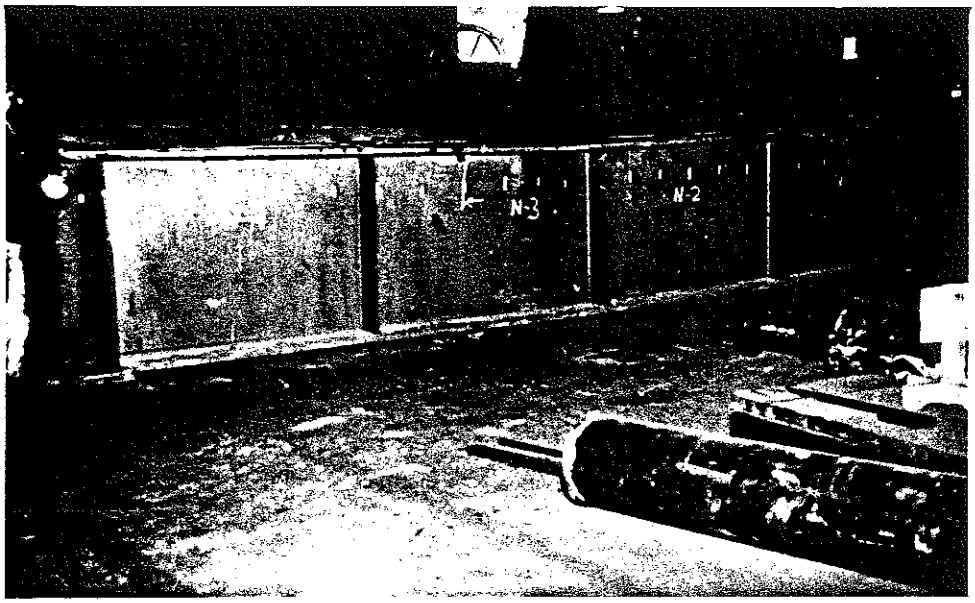


(a)

Fig. 3 a) Crane runway girder removed from service.

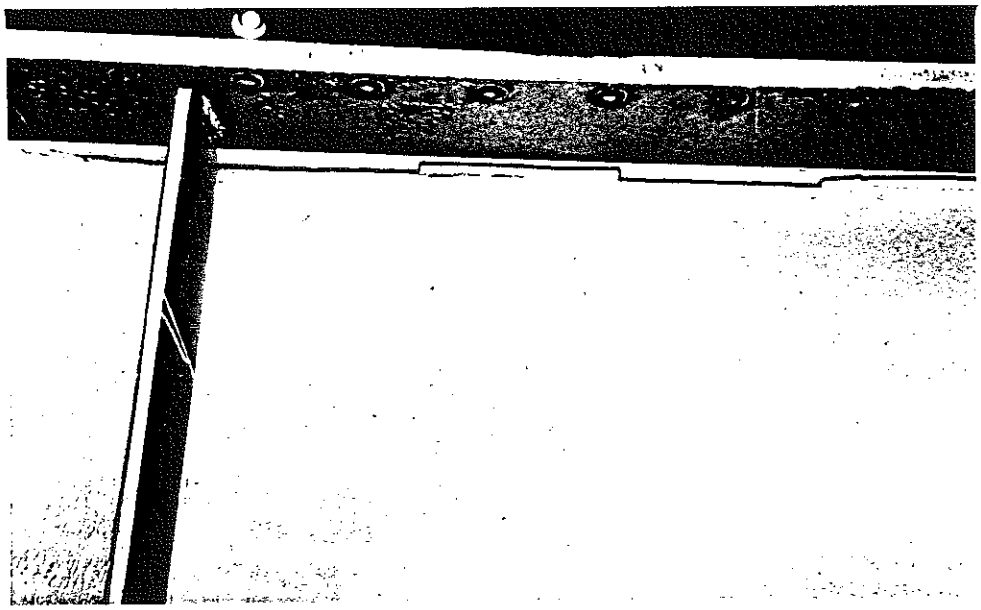

(b)

b) Detail of cracking in web-to-flange weld and in stiffener-to-flange weld.

c) Detail of web buckling beneath cracked web-to-flange weld.

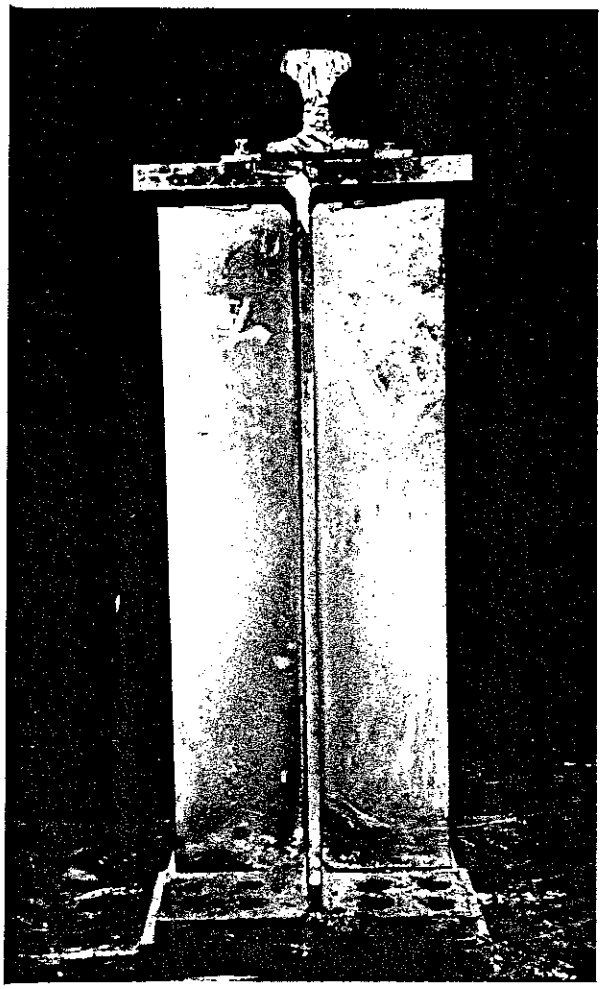

d) Eccentricity of rail relative to the web.

continuous, sometimes repeated, repairs and the necessary closing of the runway during such repairs.

The early literature proved that it was local, wheel-load-induced cyclic stresses, and not the global girder bending stresses, which, in combination with residual stresses from the various welds, cause the observed cracking. Each trolley wheel transfers a vertical gravity force onto the rail which is loosely clipped to the top of the compression flange. The rail acts to distribute the load and to transfer it through contact stresses onto this flange. The flange in turn distributes and transmits the wheel load in the form of vertical compressive stress to the top of the web, as in Figure 4a. Since there are large residual tensile stresses from the welding process in the regions of observed cracking, the compressive stresses from the wheel-load create an unloading tensile stress range with each wheel passage. Additional stresses arriving at the top of the web, as in Figure 4b, are due to out-of-plane forces and torsional moments which are always present due to horizontal thrust forces, rail eccentricity (see Figure 3d), load eccentricity on the rail, and non-uniform contact conditions between the rail and the flange. These effects can induce additional cyclic compressive or tensile stress ranges in the affected weld details.

Because a trolley is supported by 4 to 8 wheels, and because of the continuous operating conditions in most mills, the number of individual wheel-induced stress cycles in crane runway girders mounts rapidly. The combination of rapid load cycle accumulation with apparently high local stress ranges causes cracking to occur in heavily loaded girders at an unexpectedly early time in their lives.

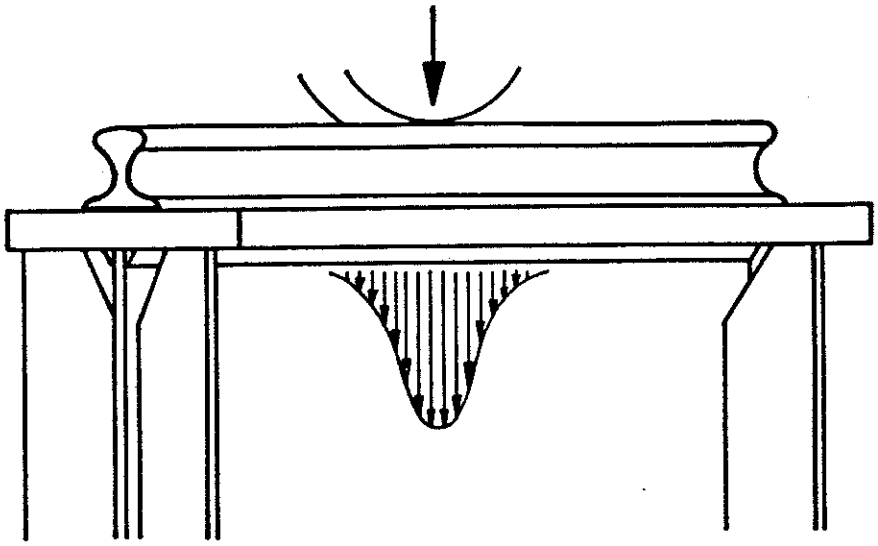

(a)

Fig. 4 Schematic of vertical stress distributions along the top of the web. a) From vertical wheel load; b) From factors causing torsion of rail-flange assembly.

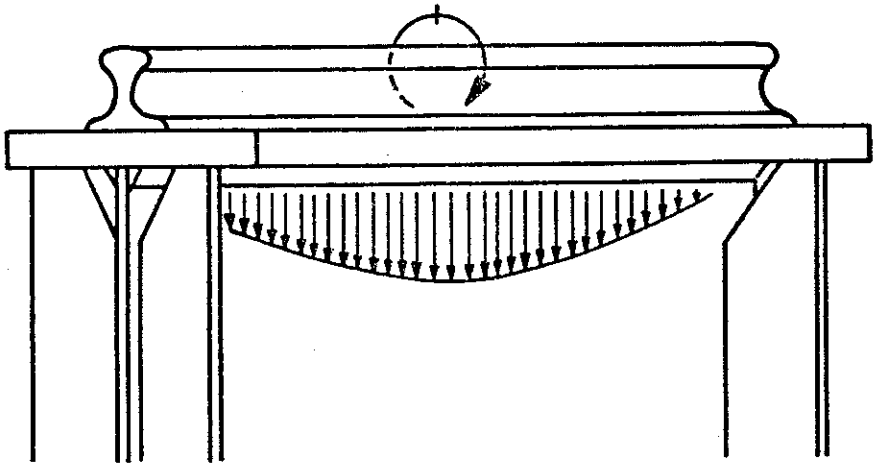

(b)

Considerable research has been performed in both Europe and the U.S. during the 1960's and 1970's in response to this problem.[1] In the U.S. major studies were undertaken by a number of steel producers. Significant results of these included recommendations to use a full-penetration weld for the web-to-flange connection, to use deep copes on the vertical stiffeners, and to attach the stiffeners to the bottom of the compression flange using a full-penetration weld. Some of these recommendations have evolved into today's recommended practice. Still, as of the 1979 edition of the Association of Iron and Steel Engineers' (AISE) Technical Report No. 13, "Guide for the Design and Construction of Mill Buildings," there were no recommended methods by which a designer could minimize the likelihood of fatigue cracking in runway girders.

The only relevant analytical information available to a designer using Technical Report No. 13 is its recommendation in Section 5.8.7 that,

$$\sigma_{yy_{avg}} = \frac{P}{2(d + t_f)\ t} \qquad (1)$$

As can be seen from Figure 5, this expression is an approximation for the average vertical normal stress arriving at the top of the web due to a concentric vertical wheel load. The important specific questions left unanswered by the 1979 edition of Technical Report No. 13 were:

1. How accurate is the above equation? Is there a significant difference between the average values of $\sigma_{yy}$ estimated by this equation and the peak value calculated by vigorous analytical methods?

[1] A complete bibliography is attached as Appendix I, "A Bibliography on Fatigue in Crane Runway Girders"; Commentary on major works is contained in Appendix III, "Fatigue Cracking in Compression Zones of Crane Runway Girders: Part 1 - Literature Review."

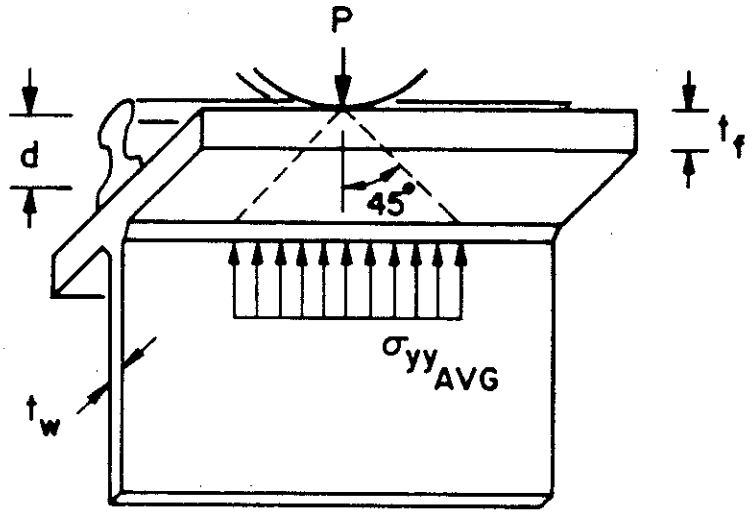


Fig. 5 Schematic of average stress distribution implied by Equation 1.

2. How significant are the additional components of $\sigma_{yy}$ due to the out-of-plane effects previously mentioned?
3. How effective is the use of an elastomeric pad placed between the rail and the flange in reducing $\sigma_{yy_{max}}$?
4. What is the effectiveness of intermediate vertical stiffeners in reducing $\sigma_{yy_{max}}$? What stress range is induced in the stiffener-to-flange weld?
5. Given a method of computing the combined maximum stress range, $\sigma_{yy_{max}}$, what is the resistance of the detail to crack initiation? If it is a partial penetration weld? If it is a full penetration weld? Is S-N data available for such details, and if so, what are its origin and applicability?
6. Given the observation that initiation of cracking type A is not synonymous with failure, that is, that there are a significant number of load cycles required to propagate an initiated crack to a length which causes failure, what rate-of-growth can be expected?

## 2. The AISE/Cornell Crane Runway Girder Project

Early in 1983, the AISE issued a request for proposals to research and answer the above questions. The ultimate objective of the requested study would be to produce analytical tools and resistance information which could be included in the recommended procedures for design of those girders which are contained in AISE's Technical Report No. 13. A proposal from Cornell University was accepted and a research project began in July of 1983. This project was divided into the four principal tasks indicated in Table 1.

Table 1

Overview of AISE/Cornell Crane Runway Girder Project

Task I. Information Retrieval

Task II. Numerical Modeling

Task III. Physical Testing

Task IV. Report Preparation

The kernel of the project was the development of analytical methods for predicting the stress range in the web-to-compression-flange weld detail. This was the primary objective of Task II, Numerical Modeling. A number of constraints was placed on this objective:

- The end product had to be in a form usable by design engineers. Although the most sophisticated finite and boundary element techniques were to be employed during their development, simple expressions or graphs were to be made available for potential inclusion in AISE TR No. 13.
- The proposed analytical solutions had to undergo comprehensive comparison with any existing related solutions available in any literature. Potential differences had to be explained, and theoretical accuracies evaluated. Those comparisons were to be based on the efforts in Task I, Information Retrieval.
- The proposed analytical solutions had to be critically evaluated by means of comparison with results from full-scale physical testing, the content of Task III.

Comprehensive interim reports containing details of major components of each task were also scheduled as Task IV. Table 2 presents a list of these reports by date of publication within each task.

Table 2

Interim Reports Completed Under the AISE/Cornell
Crane Runway Girder Project

---

Task I: Information Retrieval

Report No. 1: "A Bibliography on Fatigue in Crane Runway Girders," by K. Mettam, A. R. Ingraffea, and W. H. Gerstle, January 9, 1986, 22 pp.

Task II: Numerical Modelling

Report No. 1: "Numerical Modelling of Forces Transmitted to the Web-to-Flange Junction of Crane Runway Girders Due to Wheel Loads," by W. H. Gerstle and A. R. Ingraffea, May 15, 1984, 108 pp.

Report No. 2 "Effects of Elastomeric Rail Pad on Forces Transmitted to the Web-to-Flange Junction of Crane Runway Girders," by A. R. Ingraffea and S. C. Lin, March 5, 1985, 46 pp.

Report No. 3 "The Effect of Stiffeners on the Forces Transmitted to the Web-to-Flange Junction of Crane Runway Girders," by P. Wawrzynek and A. R. Ingraffea, January 20, 1985, 50 pp.

Report No. 4 "Stress Intensity Factor Solutions and Crack Propagation Studies for Flaw Growth in the Web-to-Flange Weld Detail," by W. H. Gerstle, January 8, 1986, 220 pp.

Task III: Physical Testing

Report No. 1 "Fatigue Cracking in Compression Zones of Crane Runway Girders: Part 1 - Literature Review; Part 2 - Outline of Cornell Experimental Studies," by K. Mettam, January 14, 1985, 75 pp.

Report No. 2 "An Experimental Investigation of Fatigue Cracking in Welded Crane Runway Girders Due to Wheel Induced Stresses," by K. Mettam, January 8, 1986, 192 pp.

The first objective of this project final report is to summarize the conclusions and recommendations from each task. The interim reports generated by each task are attached to this report as appendices. The second objective of this report is to make final recommendations with regards to fatigue design of the top flange-to-web detail. These are accompanied by example problems.

## 3. Summary of Task I: Information Retrieval

Appendix I contains Task I, Report #1 entitled "A Bibliography on Fatigue in Crane Runway Girders." This report contains over 50 references specifically addressing fatigue in crane runway girders, and also cites nearly 70 closely related papers and reports. The references are categorized as "on-file," meaning that a copy is contained in the Project Library, or as "searching," meaning that, as of the end of the project, a copy could not be located.

A review of the available literature is contained in Appendix III in Part 1 of Task III, Report No. 1. One of the most important products of the literature search was the discovery in various European design standards of S-N category curves and fatigue-limit stress ranges for the flange-to-web weld detail (these are presented later in Section 7). The origin of these curves and limiting stresses was pursued vigorously with the objective of obtaining answers to the following questions:

1. Are they based on actual fatigue testing or are they based on judgement and experience?
2. What constitutes "failure"?

Despite numerous telegrams, phone calls, and letters, those questions could not be answered within the time frame of this project. It is recommended that AISE Subcommittee No. 13 continue to pursue these important questions.

## 4. Summary of Task II: Numerical Modeling

Three interim reports were generated by Task II. These are attached in Appendix II and summarized here.

### 4.1 Task II, Report #1: Numerical Modeling of Forces Transmitted to the Web-to-Flange Junction of Crane Runway Girders Due to Wheel Loads

This report contains the foundations of the analytical effort on this project. The most important results reported here are three analytical expressions for the vertical normal stress, two for vertical wheel load and one for torsion of the top flange. The two expressions for stress due to vertical wheel load account for the extremes of point and uniform contact the rail and the flange. These three expressions are the most important result of the entire project and received continuous scrutiny and re-evaluation. Specific conclusions reached in this report are:

> "A parameter study has been reported which predicts the influence of flange thickness, flange width, and web thickness on the vertical force per unit length and the moment per unit length transmitted from the top flange to the web of a crane runway girder. Influence functions (kernel functions) have been developed which give the forces in the web-to-flange junction caused by point loads applied to the top of the flange. By integrating the kernel functions with respect to an applied traction to the flange, the forces transmitted to the web-to-flange junction can be calculated.
>
> The vertical normal stresses between the web and top flange were determined through the use of two-dimensional plane stress finite element analyses. By varying web thickness and flange width, eighteen separate girder geometries were considered. A convergence study showed that the results of these analyses were reliable.

The moment per unit length between the web and flange resulting from an applied point moment was determined through the use of a Fourier series plate analysis program especially written for the task. Again, eighteen different girder geometries were analyzed. The results were checked with a finite element analysis using SAP6. A study was conducted to determine how many terms had to be included in the Fourier series to guarantee convergence.

Two different formulas were generated using curve fitting techniques to approximate the kernel functions as a function of flange thickness, flange width, and web thickness. These formulas give accurate approximations of the vertical normal stress and the moment per unit length caused by an applied concentric point load and an applied moment to the top flange, respectively.

Finally, knowing these kernel functions and the applied traction components to the top flange, the resulting nominal stresses between the web and the flange could be calculated by integration. An example problem was presented.

The kernel function for an applied concentric point load to the top flange was found to be

$$K_\sigma = \left(\frac{.65}{t_w t_f}\right)\left(\frac{b_f}{t_w}\right)^{-.288} \exp^{-1.327\left(\frac{t_w}{b_f}\right)^{.576}\left(\frac{x}{t_f}\right)^2} \qquad \text{(Eq. 3.26)}$$

The kernel function for an applied moment about the longitudinal axis of the top flange was found to be

$$K_M = \left[\frac{1}{\sqrt{4\pi}} \exp^{-(Dx/GK)}\right] \Big/\Big/ \sqrt{\frac{GKx}{D}} \qquad \text{(Eq. 3.27)}$$

Both of these kernel functions are only correct if the applied wheel loads are "far" from the ends of the girder or from a vertical stiffener.

The vertical normal stress $\sigma_{yy}$ between the flange and the web is given by

$$\sigma_{yy} = \int_{-\infty}^{\infty} V(t)K_{\sigma}(t - x)\, dt \qquad \text{(Eq. 3.28)}$$

The moment per unit length $m_{yy}$ between the flange and the web is given by

$$m_{yy} = \int_{-\infty}^{\infty} M(t)K_{M}(t - x)\, dt \qquad \text{(Eq. 3.29)}$$

With the aid of these analysis formulas, it will be possible to calculate the stresses in the weld between the web and the flange in a simplified manner."

## 4.2 Task II, Report #2: Effects of Elastomeric Rail Pad on Forces Transmitted to the Web-to-Flange Junction of Crane Runway Girders

This report contains analytical verification of the stress-reduction effects of elastomeric rail pads. Of particular importance are the results which indicate that stress-reduction of over 50% is theoretically attainable. Specific conclusions and recommendations reported include:

"The following conclusions were drawn on the basis of the analysis results reported here:

1. Rail uplift tends to increase the peak vertical stress transmitted to the web. An analysis method which does not permit uplift and its attendant stress redistribution will underestimate this stress. For the problem considered in this report, the non-linear analysis which modeled uplift predicted a peak stress 11 percent higher than that predicted by a linear analysis which assumed that the rail was rigidly connected to the flange.
2. Longitudinal shear transfer between the rail and the flange has a substantial influence on the peak vertical stress transmitted to the

web. As shear transfer decreases, the transmitted stress increases. For the problem considered in this report, a bounding frictionless condition between the rail and the flange produced a 17 percent higher peak stress than that predicted using a bounding shear-locked condition.

3. The inclusion of a steel wear plate between the rail and the flange has a negligible effect on decreasing the peak vertical stress transmitted to the web.
4. The inclusion of an elastomeric rail pad between the rail and the stiffener reduces the peak value of the vertical stress transmitted to the web.
5. The normal stiffness of elastomeric pad material is a strong function of the normal stress on the pad. As the normal stress increases, the pad stiffens, and the capability of the pad to reduce web stress decreases.
6. For the particular pad material and girder geometry used in the present study, the reduction factor in the peak vertical stress transmitted to the web ranged from 66 to 28 percent for wheel loads ranging from 1 kip to 100 kips, respectively.
7. The reduction factor of 50 percent currently recommended by some codes and designers can only be justified, for a given pad material, over a limited range of wheel loads. For the pad material and girder geometry used here, a 50 percent reduction factor would be justifiable only for wheel loads less than about 60 kips.

## 5.2 Recommendations

It is beyond the scope of this report to recommend or not to recommend the use of elastomeric rail pads. Such a recommendation

should come only as a result of a total cost-effectiveness study. The principal considerations in such a study must include:

- The initial cost of pad material and its installation
- The cost of maintaining the pad in proper working order
- The savings in girder repair or replacement costs which might accrue as a result of increased longevity due to pad usage.

The impact of the results of this report should be felt in each of those considerations. The initial cost of a pad is related to its design, and its design to the working stress. The analyses presented here indicate that, for the typical girder design employed, peak normal stress in the pad can be as high as 2700 psi for a 100 kip wheel load. This stress level might be at the extreme high end of the useful range for the particular pad material used.

The cost of maintaining the pad must depend on its wear and fatigue lives. These of course depend on the normal and shear stresses which the pad must transfer it. Practice and the current results indicate that considerable shear motion, both longitudinal and lateral, occurs between the rail and the flange. The effect of this relative motion, under high normal stress, must be considered in assessing the wear life of a pad.

Finally, the key issue in assessing potential savings by increasing girder life is the stress-range reduction factor. It has been shown clearly in this report that substantial reduction factors can be obtained through the use of a pad. Since fatigue life is inversely related to stress range raised to a power greater than one, even a modest decrease in stress-range can result in a substantial increase in fatigue life. However, it has also been shown, for the first time rigorously, that the

reduction factor depends strongly on the applied wheel load and on the particular pad material in use. The reduction factor of 50 percent suggested by Gorenc (13) and Senior and Gurney (4) cannot be recommended for use in all instances. The lowest value of reduction factor found in the present study, about 29 percent might well be too high for higher wheel loads on the pad studied here, or for lower loads on a different pad. The current AISE recommendation, that "appropriate finite element analysis" be used to assess the effect of rail pads, is still well advised. It is recommended here, however, that the word "appropriate" be more clearly defined to mean an analysis in which non-linear pad behavior is rigorously included."

### 4.3 Task II, Report #3: The Effects of Stiffeners on the Forces Transmitted to the Web-to-Flange Junction of Crane Runway Girders

The literature review and the analyses described in Report #1 both indicated that the vertical stress component caused by flange torsion is not negligible. This report highlights the role played by intermediate vertical stiffeners in controlling flange torsion. It also re-evaluated the analytical expressions for vertical stress components developed in Report #1 and led to their final form. Specific conclusions drawn in this report were:

"The primary objective of this report is to present modifications to Equations C-1 and C-2 presented in Report 1 to allow for the presence of intermediate vertical stiffeners. A number of secondary objectives were included in the investigation. The investigation was performed in three stages. First, a complete girder was modeled to investigate the extent of localized girder behavior. This information was used to decide what portion of the girder should be modeled with a more refined finite element mesh. The second stage of the investigation was an examination of the effects of a vertical load on the force transmitted to the web. In

the final stage a study was made of the effects of a lateral load on the moment transmitted to the web, using a more refined mesh than was employed in stage one.

For the case of a vertical load applied to the top of the rail three finite element analyses were presented. The three analyses correspond to the configurations of the load applied at mid-panel, six inches from the stiffener plane, and in the stiffener plane. It was observed that as the load moves toward the stiffener there is some reduction in the maximum stress in the web. For this geometry the reduction in vertical stress when the load is in the stiffener plane is about 15 per cent. It was also observed that as the load moves away from the stiffener plane this reduction in stress dissipates rapidly.

The finite element results were found to give a maximum vertical stress which is about 40 per cent less than the result given by Equation C-1. This discrepancy is explained by the nature of the assumptions implicit in the two analyses. Equation C-1 assumes that the rail sits on a rigid foundation. A real rail sits on an elastic foundation so that case Equation C-1 gives an upper bound value for the maximum stress in the web. Further, the finite element analysis assumes that there is no slip of the rail relative to the flange. It was shown that for the magnitude of the shear stress at the rail-to-flange interface, and for the frictional resistance available, slippage can occur. Because of this the finite element analysis gives a lower found value for the stress in the web.

For the case of a lateral load it was found that the critical point of load application is when the load is mid-way between stiffeners. It was shown that for a girder with no intermediate stiffeners the effect of the lateral load dissipates over the full length of the girder. When stiffeners

are provided the effect of the lateral load has dissipated by a distance of one stiffener spacing from the point of load application.

A comparison was made between the maximum moments predicted by Equation C-2 and the finite element results reported in Chapter 2. There was a significant discrepancy between these two values. The primary reason for this discrepancy was that Equation C-2 ignores the torsional stiffness of the rail. It was observed from the finite element results that the torsional stiffness of the rail plays an important role in the behavior of the uppermost part of the girder. It was also noted that the rigid foundation assumption in Equation C-2 causes an increase in the magnitude of the maximum moment transmitted to the web.

It was observed that for the case of a girder with stiffeners the maximum moment was reduced by 45 per cent when the load was applied at mid-panel and by 77 per cent when the load was applied in the stiffener plane."

## 4.4 Report #4: Stress-Intensity Factor Solutions and Crack Propagation Studies for Flaw Growth in the Web-to-Flange Weld Detail

This report is part of a doctoral thesis entitled: "Finite and Boundary Element Modeling of Crack Propagation in Two- and Three-Dimensions Using Interactive Computer Graphics." The most important result of this study is the development of a procedure to predict analytically the rate of growth of a flaw in the web toe of the web-to-flange full penetration weld. Although theoretically rigorous, this procedure would require substantial refinements before it could be used for practical design. Ultimately, it could replace the S-N approach as a fatigue design tool.

## 5. Summary of Task III: Physical Testing

Two interim reports were generated by Task III. These are attached in Appendix III.

### 5.1 Task III, Report #1: Fatigue Cracking in Compression Zones of Crane Runway Girders: Literature Review and Outline of Cornell Experimental Studies

The first four chapters of this report contain the detailed literature review alluded to in Section 2, above. Chapter 5 and Appendices describe the physical testing program for the project. This includes specimen and test frame design, and a testing schedule.

### 5.2 Task III, Report #2: An Experimental Investigation of Fatigue Cracking in Crane Runway Girders Due to Wheel Induced Stresses

This report contains descriptions and results of the physical tests performed on the project. Its key elements are:

1. The experimental verification of the stress analyses reported in the Task II reports.
2. The observations of the important effects of the contact condition between the rail and the flange on stress transmission.
3. The experimental verification of the theoretically predicted stress reduction due to elastomeric rail pads.
4. The observation, apparently for the first time, of a propagating crack in the web toe of a full-penetration-welded detail of a full-scale girder.
5. The observation that, under vertical concentric load alone, such cracking was relatively slow, about $1.5 \times 10^{-7}$ in/cycle at the web surface at a stress range of 30 ksi.
6. The observation that, although this crack grew in length from 1/4 in to about 5/8 in on the web surface in 3.6 million wheel cycles, it did not break through the 1/2 in thick web.

6. Verification of Results

As previously noted, the most important results of this project are the analytical expressions for the stresses transmitted to the web due to wheel loading. The expression for the maximum vertical normal stress transmitted to the web due to a concentric wheel load, and under the assumption of uniform contact between the rail and the flange, is,

$$\sigma_{yy_{max}} = \frac{\left(\frac{0.65P}{tt_f}\right)\left(\frac{b_f}{t}\right)^{-0.29}}{\sqrt{1 + \frac{1.33}{\alpha}\left(\frac{t}{b_f}\right)^{0.58}\left(\frac{d}{t_f}\right)^2}} \qquad (2)$$

where,

P = applied wheel loads, kips

t = web thickness, in.

$t_f$ = flange thickness, in.

$b_f$ = flange width, in.

d = rail height, in.

$\alpha$ = rail foundation stiffness factor

For point contact between the rail and the flange,

$$\sigma_{yy_{max}} = \left(\frac{0.65P}{tt_f}\right)\left(\frac{b_f}{t}\right)^{-0.29} \qquad (3)$$

The maximum bending moment per-unit-length transmitted to the top of the web due to applied torsional momemt M applied to the rail/flange assembly can be obtained from Figure 6, wherein,

G = shear modulus of elasticity, ksi

K = sum of torsional constants of the rail and the flange, $in^4$

D = web plate flexural rigidity, kip-in

a = stiffener spacing, or span, in

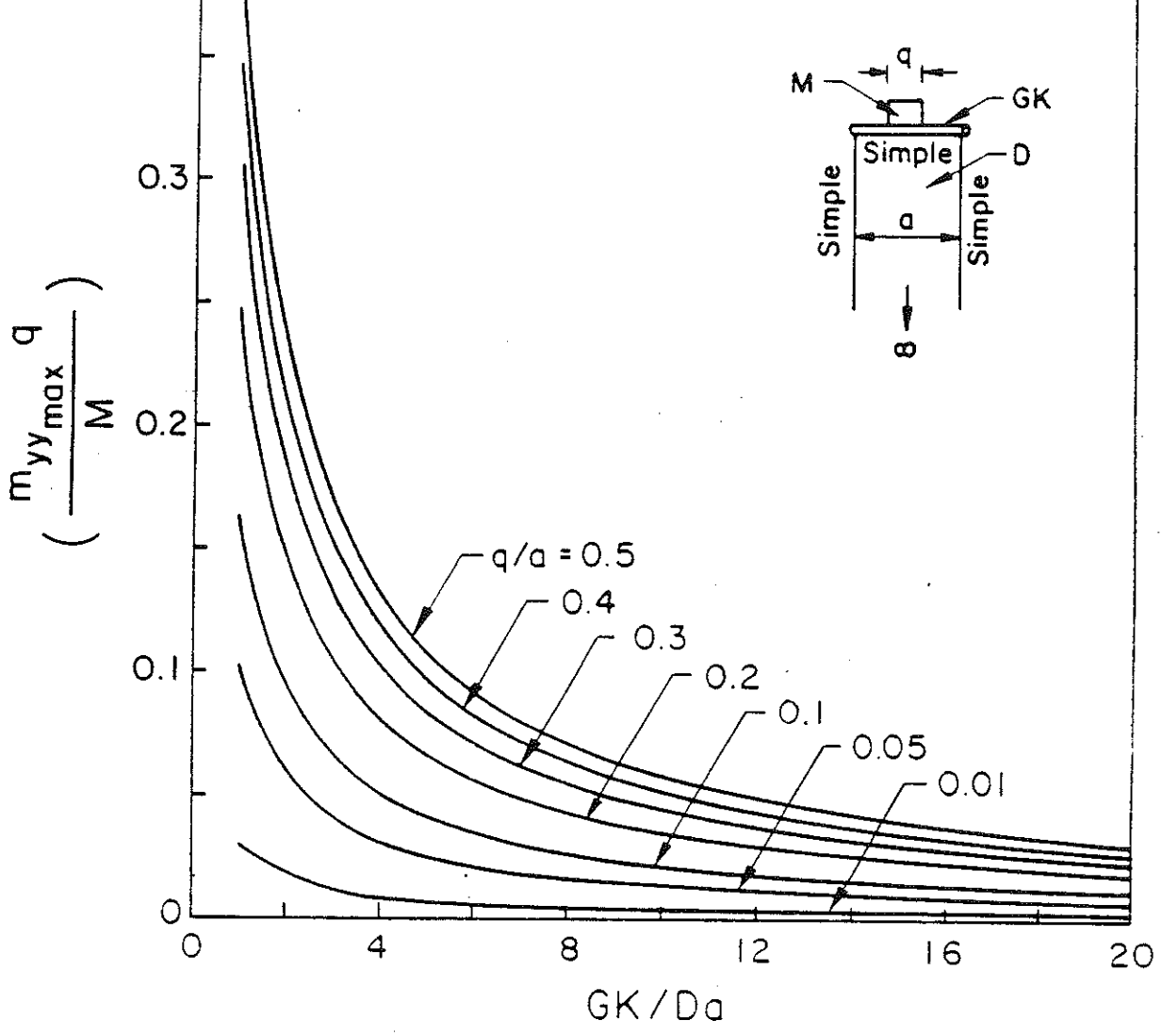


Fig. 6 Maximum moment per-unit-length transmitted to top-of-web, $m_{yy_{max}}$, due to a torsional moment, M, applied to the rail/flange assembly. a) For girders with intermediate vertical stiffeners welded to the top flange. Stiffener spacing is a.

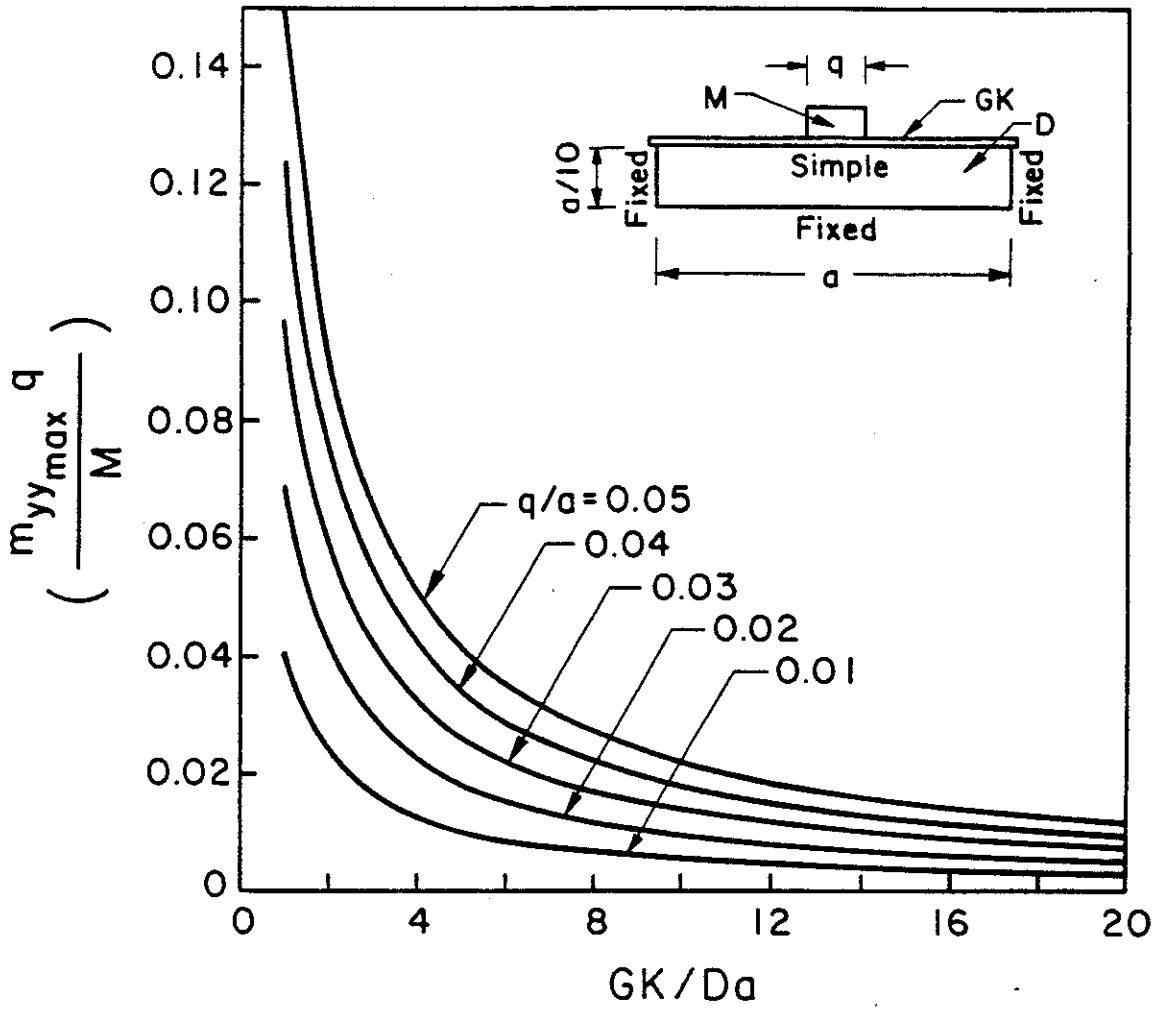


Fig. 6 b) For girders without intermediate vertical stiffeners, or with stiffeners not welded to the top flange. Girder span is a.

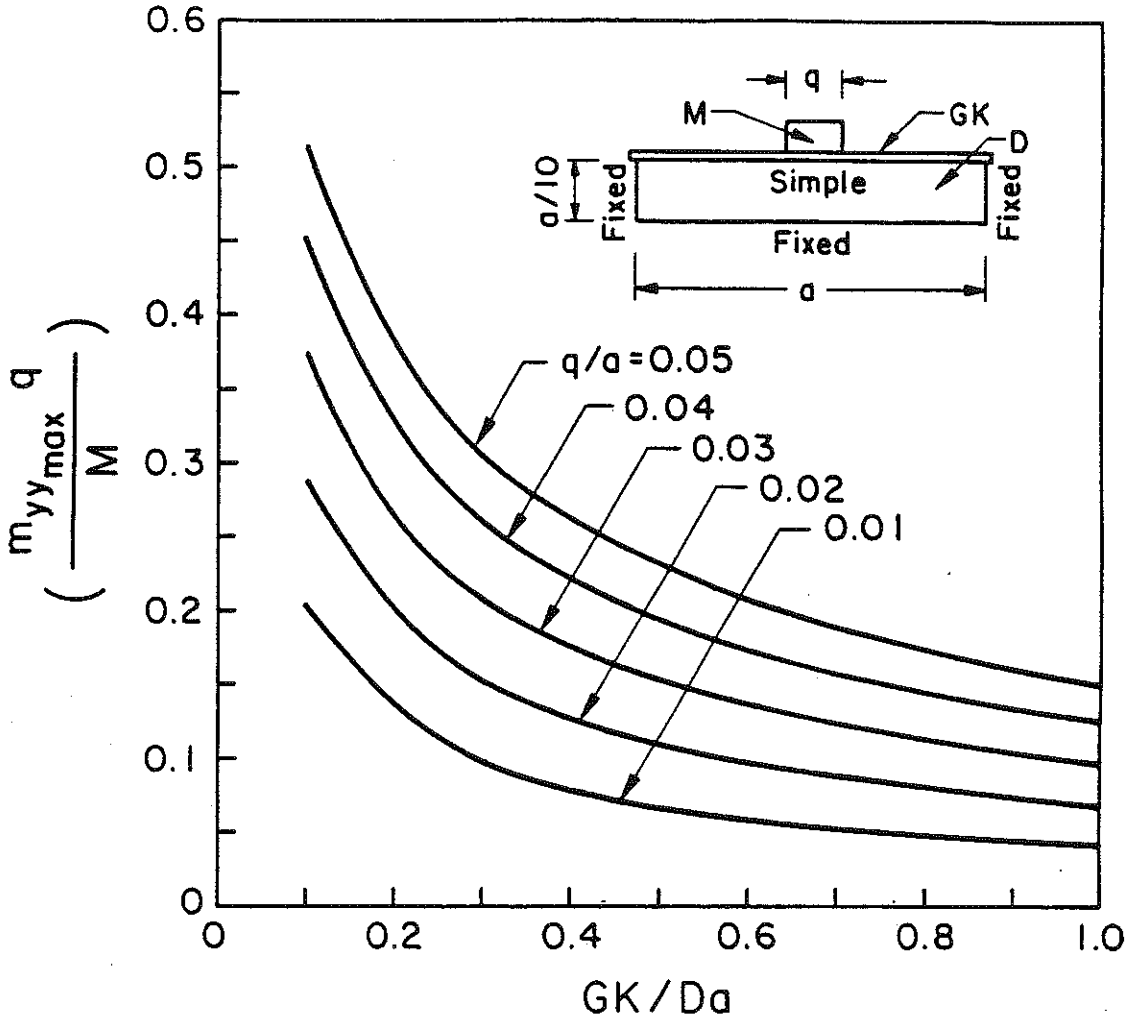


Fig. 6 c) As in Fig. 1b, but horizontal scale expanded in the range $\frac{GK}{Da} \leq 1$.

Figure 6a is applicable only to the case in which the girder has intermediate vertical stiffeners which are welded to the top flange. Figure 6b is for girders without intermediate stiffeners, or with stiffeners which are not welded to the top flange. For either of these latter two cases, the symbol a in Figure 6b represents the girder's span. Although the results shown in Figure 6b were obtained for a span-to-depth ratio of 10, error in their use for any other common ratio would be negligible.

These results were obtained through multi-step processes with verification, both analytical and physical, performed at a number of points in their development. A description of their evolution and verification follows.

6.1 Equations 2 and 3: Evolution and Verification

The development of Equations 2 and 3 began in the work contained in Task II, Report #1. In that report Equation 3 is the fundamental solution, or kernel function, used to obtain Equation 2 which appears finally as Equation C-1 in Appendix C of that report. It is based on dimensional analysis and finite element analysis. The first external verification of those equations came with the discovery of the work by Parkes who, using classical principles of structural mechanics, derived almost identical results. Both the Parkes equation and the original version of Equation 2 assumed that the rail rested on a rigid foundation. Work reported in Task II, Report #3 indicated that this assumption leads to gross overestimation of $\sigma_{yy_{max}}$. The only difference between the original and final versions of this equation, C-1 of Report #1 and the present Equation 2, is the $\alpha$-term. For a rigid web, $\alpha = 2.1$, the value used in Equation C-1. For any real web, $\alpha < 2.1$. Figure 7 shows the variation in $\alpha$ with web thickness computed by finite element analysis.

Additional verification of Equation 2 was obtained from physical testing. Table 3 compares measured stresses for four girder geometries with finite

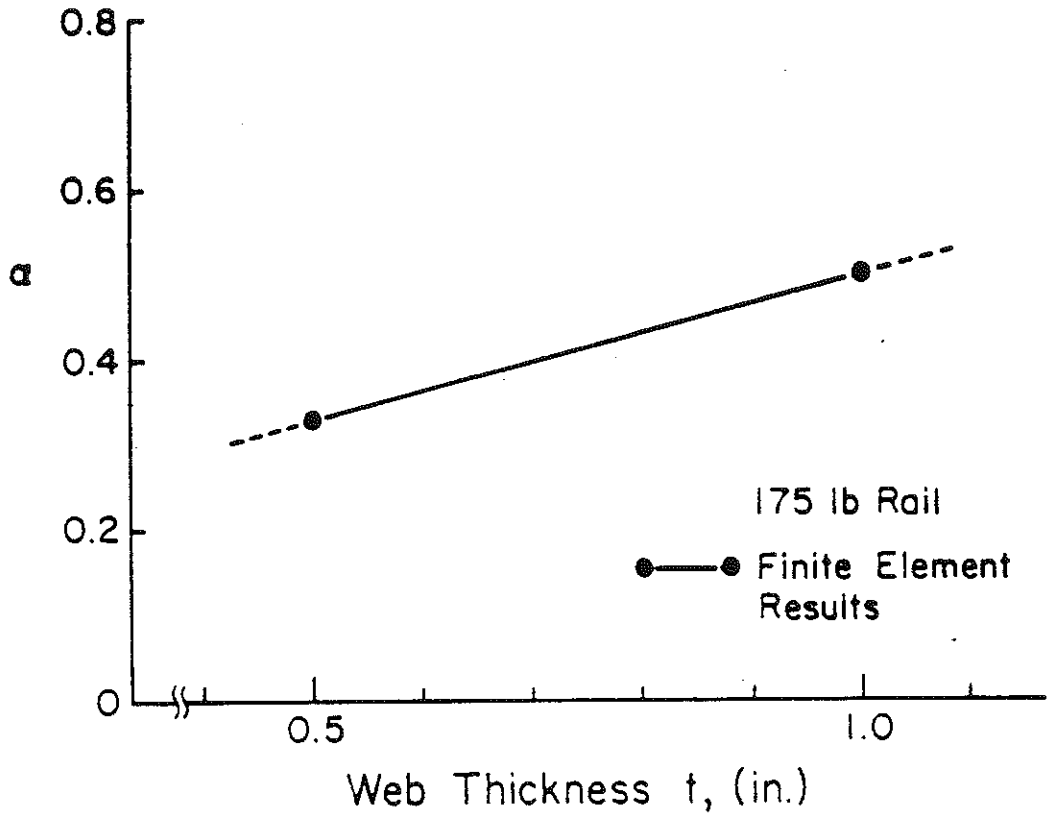


Fig. 7 Rail foundation stiffness factor, α, for use in Equation 1, as a function of web thickness.

TABLE 3: COMPARISON OF VALUES FOR VERTICAL STRESS TRANSMITTED TO WEB DUE TO 100 KIP CONCENTRIC WHEEL LOAD (from Task III, Report #2)

| Geometry[c] | | Vertical Stress[d] Transmitted to Web (ksi) | | | | | | |
|---|---|---|---|---|---|---|---|---|
| | | At Web/Flange Connection | | | | | At Strain Gage Locations | |
| t (in.) | $t_f$ (in.) | AISE[8] Sect. 5.8.7 | Senior & Gurney[1] | Equation 4 $\alpha$ = 2.11 | Equation 4 Modified | 3-D Finite Element | 3-D Finite Element | Experiment |
| 1 | 2.5 | 5.9 | 7.1 | 8.5 | 5.7[a] | 5.3 | 4.8 | 4.5 |
| 1 | 1.5 | 6.7 | 8.4 | 11.0 | 6.2[a] | 6.2 | --- | --- |
| 1 | 1 | 7.1 | 8.9 | 12.0 | 6.5[a] | 6.7 | 6.0 | 7.4 |
| .5 | 2.5 | 11.8 | 11.3 | 15.0 | 9.2[b] | 8.6 | 8.1 | 8.5 |
| .5 | 1.5 | 13.3 | 13.3 | 20.2 | 10.1[b] | 10.1 | --- | --- |
| .5 | 1 | 14.3 | 14.2 | 23.2 | 10.5[b] | 10.9 | 10.3 | 11.1 |

[a] $\alpha$ = .50

[b] $\alpha$ = .33

[c] all geometries include $b_f$ = 20 in., b = 72 in., a = 72 in.

[d] all are peak values except first column which contains average values

element predictions at strain gage locations. Agreement is generally very good. Since Equation 2 predicts stress at the top of the web and not at strain gage locations, direct comparison with measurements is not meaningful or possible. However, Table 3 also shows a comparison of Equation 2 predictions with finite element calculations at the top of the web. This comparison is also very good, with a maximum difference of less than 8%.

Table 4 shows additional comparisons with other analytical solutions. Equation 2 is consistently lower than all other solutions because of its account of finite web stiffness.

6.2 Figure 6: Evolution and Verification

The results shown in Figure 6 are also based on developments described in Task II, Report #1. Their basis is classical, coupled plate-torsional beam theory which produced an analytical result in the form of an infinite series. These results are obtained by evaluating the first 1000 terms of the infinite series solution for the structures shown in Figures 6a and 6b. The moment applied to this structure, M, is assumed to be uniformly distributed over a length q. Based on St. Venant's principle, q should be at least 2 times the rail height, d. Three-dimensional finite element results indicate that q is about 5 times d. However, as can be verified (see Example Problem #1, below) by example, $m_{yy_{max}}$ values from Figure 6 are relatively insensitive to the value of q.

The literature review produced other solutions for $m_{yy_{max}}$. Reviews and critiques of these solutions are given in Task II, Report #1 and Task III, Report #2. Table 5 presents a summary of comparisons of the predictions of Figure 6a with other solutions.

Physical testing also gives verification to the present solution. Table 6 again shows the indirect comparisons, physical test results to finite element,

Table 4 : Comparison of Equations for Vertical Web Stress due to Vertical Loading (from Task III, Report #2)

| $t$ (in) | $t_f$ (in) | $b_f$ (in) | AISE* EQN (ksi) | Predicted Peak Stress/AISE* Cornell Solution | Senior &Gurney | Gorenc | Girkman |
|---|---|---|---|---|---|---|---|
| 0.5 | | | | | | | |
| | 0.5 | | | | | | |
| | | 10.0 | 15.38 | 0.70 | 0.97 | 1.00 | 0.76 |
| | | 20.0 | 15.38 | 0.70 | 0.97 | 1.00 | 0.76 |
| | | 30.0 | 15.38 | 0.70 | 0.97 | 1.00 | 0.76 |
| | 1.0 | | | | | | |
| | | 10.0 | 14.29 | 0.74 | 0.99 | 1.07 | 0.82 |
| | | 20.0 | 14.29 | 0.73 | 0.99 | 1.07 | 0.82 |
| | | 30.0 | 14.29 | 0.73 | 0.99 | 1.06 | 0.82 |
| | 1.5 | | | | | | |
| | | 10.0 | 13.33 | 0.78 | 1.00 | 1.14 | 0.88 |
| | | 20.0 | 13.33 | 0.76 | 1.00 | 1.13 | 0.88 |
| | | 30.0 | 13.33 | 0.75 | 1.00 | 1.11 | 0.88 |
| | 2.0 | | | | | | |
| | | 10.0 | 12.50 | 0.80 | 0.99 | 1.19 | 0.94 |
| | | 20.0 | 12.50 | 0.78 | 0.99 | 1.16 | 0.94 |
| | | 30.0 | 12.50 | 0.76 | 0.99 | 1.13 | 0.94 |
| | 2.5 | | | | | | |
| | | 10.0 | 11.76 | 0.82 | 0.96 | 1.24 | 1.00 |
| | | 20.0 | 11.76 | 0.78 | 0.96 | 1.18 | 1.00 |
| | | 30.0 | 11.76 | 0.76 | 0.96 | 1.13 | 1.00 |
| 1.0 | | | | | | | |
| | 1.0 | | | | | | |
| | | 10.0 | 7.14 | 0.91 | 1.25 | 1.35 | 1.04 |
| | | 20.0 | 7.14 | 0.90 | 1.25 | 1.35 | 1.04 |
| | | 30.0 | 7.14 | 0.90 | 1.25 | 1.34 | 1.04 |
| | 2.0 | | | | | | |
| | | 10.0 | 6.25 | 0.99 | 1.25 | 1.51 | 1.18 |
| | | 20.0 | 6.25 | 0.96 | 1.25 | 1.46 | 1.18 |
| | | 30.0 | 6.25 | 0.93 | 1.25 | 1.43 | 1.18 |
| | 2.5 | | | | | | |
| | | 10.0 | 5.88 | 1.01 | 1.21 | 1.56 | 1.26 |
| | | 20.0 | 5.88 | 0.96 | 1.21 | 1.48 | 1.26 |
| | | 30.0 | 5.88 | 0.93 | 1.21 | 1.42 | 1.26 |
| | 3.0 | | | | | | |
| | | 10.0 | 5.56 | 1.03 | 1.16 | 1.59 | 1.33 |
| | | 20.0 | 5.56 | 0.97 | 1.16 | 1.48 | 1.33 |
| | | 30.0 | 5.56 | 0.92 | 1.16 | 1.39 | 1.33 |
| | 4.0 | | | | | | |
| | | 10.0 | 5.00 | 1.04 | 0.98 | 1.61 | 1.48 |
| | | 20.0 | 5.00 | 0.95 | 0.98 | 1.43 | 1.48 |
| | | 30.0 | 5.00 | 0.90 | 0.98 | 1.31 | 1.48 |
| | 5.0 | | | | | | |
| | | 10.0 | 4.55 | 1.04 | 0.72 | 1.58 | 1.63 |
| | | 20.0 | 4.55 | 0.93 | 0.72 | 1.35 | 1.63 |
| | | 30.0 | 4.55 | 0.86 | 0.72 | 1.21 | 1.63 |
| 1.5 | | | | | | | |
| | 1.5 | | | | | | |
| | | 10.0 | 4.44 | 1.10 | 1.44 | 1.64 | 1.27 |
| | | 20.0 | 4.44 | 1.08 | 1.44 | 1.62 | 1.27 |
| | | 30.0 | 4.44 | 1.06 | 1.44 | 1.60 | 1.27 |
| | 3.0 | | | | | | |
| | | 10.0 | 3.70 | 1.18 | 1.33 | 1.82 | 1.53 |
| | | 20.0 | 3.70 | 1.11 | 1.33 | 1.69 | 1.53 |
| | | 30.0 | 3.70 | 1.06 | 1.33 | 1.60 | 1.53 |
| | 4.5 | | | | | | |
| | | 10.0 | 3.17 | 1.19 | 0.99 | 1.83 | 1.78 |
| | | 20.0 | 3.17 | 1.07 | 0.99 | 1.59 | 1.78 |
| | | 30.0 | 3.17 | 1.00 | 0.99 | 1.44 | 1.78 |
| | 6.0 | | | | | | |
| | | 10.0 | 2.78 | 1.16 | 0.41 | 1.74 | 2.03 |
| | | 20.0 | 2.78 | 1.02 | 0.41 | 1.46 | 2.03 |
| | | 30.0 | 2.78 | 0.94 | 0.41 | 1.30 | 2.03 |
| | 7.5 | | | | | | |
| | | 10.0 | 2.47 | 1.13 | -.42 | 1.65 | 2.29 |
| | | 20.0 | 2.47 | 0.97 | -.42 | 1.35 | 2.29 |
| | | 30.0 | 2.47 | 0.89 | -.42 | 1.19 | 2.29 |

*AISE eqn for average vertical web stress

$$\sigma_{yy} = \frac{P}{2(d+t_f)t}$$ where P = 100 kips, d = 6 in.

Table 5 : Comparison of Equations for Vertical Web Stress due to Torsional Loading (from Task III, Report #2)

(M=100 kip-in, $b_f$=20.0 in, b=72.0 in)

| t (in) | $t_f$ (in) | a (in) | Cornell Solution (ksi) | Senior & Gurney (ksi) | Foucriat (ksi) | Baldin et.al. (ksi) |
|---|---|---|---|---|---|---|
| 0.5 | | | | | | |
| | 0.5 | | | | | |
| | | 48.0 | 3.52 | 2.60 | 2.88 | 2.29 |
| | | 72.0 | 4.33 | 5.17 | 3.07 | 3.43 |
| | | 96.0 | 4.86 | 8.52 | 3.48 | 4.57 |
| | 1.0 | | | | | |
| | | 48.0 | 2.78 | 2.04 | 2.26 | 1.79 |
| | | 72.0 | 3.43 | 4.08 | 2.41 | 2.68 |
| | | 96.0 | 3.86 | 6.82 | 2.75 | 3.57 |
| | 1.5 | | | | | |
| | | 48.0 | 1.76 | 1.28 | 1.43 | 1.12 |
| | | 72.0 | 2.19 | 2.60 | 1.53 | 1.68 |
| | | 96.0 | 2.47 | 4.43 | 1.75 | 2.24 |
| | 2.0 | | | | | |
| | | 48.0 | 1.03 | 0.75 | 0.83 | 0.65 |
| | | 72.0 | 1.28 | 1.52 | 0.89 | 0.97 |
| | | 96.0 | 1.45 | 2.63 | 1.02 | 1.30 |
| | 2.5 | | | | | |
| | | 48.0 | 0.61 | 0.44 | 0.49 | 0.38 |
| | | 72.0 | 0.76 | 0.91 | 0.53 | 0.58 |
| | | 96.0 | 0.87 | 1.58 | 0.61 | 0.77 |
| 1.0 | | | | | | |
| | 1.0 | | | | | |
| | | 48.0 | 4.50 | 3.73 | 4.10 | 3.57 |
| | | 72.0 | 5.22 | 6.45 | 4.16 | 5.36 |
| | | 96.0 | 5.60 | 8.84 | 4.43 | 7.14 |
| | 2.0 | | | | | |
| | | 48.0 | 1.90 | 1.44 | 1.60 | 1.30 |
| | | 72.0 | 2.29 | 2.76 | 1.68 | 1.95 |
| | | 96.0 | 2.54 | 4.27 | 1.87 | 2.60 |
| | 2.5 | | | | | |
| | | 48.0 | 1.16 | 0.87 | 0.96 | 0.77 |
| | | 72.0 | 1.43 | 1.70 | 1.02 | 1.15 |
| | | 96.0 | 1.59 | 2.76 | 1.15 | 1.53 |
| | 3.0 | | | | | |
| | | 48.0 | 0.74 | 0.54 | 0.60 | 0.48 |
| | | 72.0 | 0.91 | 1.09 | 0.64 | 0.71 |
| | | 96.0 | 1.03 | 1.81 | 0.73 | 0.95 |
| | 4.0 | | | | | |
| | | 48.0 | 0.34 | 0.24 | 0.27 | 0.21 |
| | | 72.0 | 0.42 | 0.50 | 0.29 | 0.32 |
| | | 96.0 | 0.47 | 0.85 | 0.33 | 0.43 |
| | 5.0 | | | | | |
| | | 48.0 | 0.18 | 0.13 | 0.14 | 0.11 |
| | | 72.0 | 0.22 | 0.26 | 0.15 | 0.17 |
| | | 96.0 | 0.25 | 0.46 | 0.18 | 0.22 |
| 1.5 | | | | | | |
| | 1.5 | | | | | |
| | | 48.0 | 3.41 | 3.18 | 3.46 | 3.36 |
| | | 72.0 | 3.78 | 4.90 | 3.36 | 5.04 |
| | | 96.0 | 3.95 | 6.12 | 3.41 | 6.72 |
| | 3.0 | | | | | |
| | | 48.0 | 1.02 | 0.79 | 0.87 | 0.71 |
| | | 72.0 | 1.23 | 1.48 | 0.91 | 1.07 |
| | | 96.0 | 1.35 | 2.24 | 1.01 | 1.43 |
| | 4.5 | | | | | |
| | | 48.0 | 0.35 | 0.26 | 0.29 | 0.23 |
| | | 72.0 | 0.43 | 0.52 | 0.31 | 0.34 |
| | | 96.0 | 0.49 | 0.86 | 0.35 | 0.46 |
| | 6.0 | | | | | |
| | | 48.0 | 0.15 | 0.11 | 0.12 | 0.10 |
| | | 72.0 | 0.19 | 0.23 | 0.13 | 0.15 |
| | | 96.0 | 0.22 | 0.39 | 0.15 | 0.20 |
| | 7.5 | | | | | |
| | | 48.0 | 0.08 | 0.06 | 0.06 | 0.05 |
| | | 72.0 | 0.10 | 0.12 | 0.07 | 0.08 |
| | | 96.0 | 0.11 | 0.21 | 0.08 | 0.10 |

TABLE 6: COMPARISON OF VALUES FOR PEAK BENDING STRESS TRANSMITTED TO WEB PER KIP-IN OF APPLIED MOMENT (from Task III, Report #2)

| Geometry[a] | | Peak Bending Stress Transmitted to Web (psi) | | | | |
|---|---|---|---|---|---|---|
| | | At Web/Flange Connection | | | At Strain Gage Locations | |
| t (in.) | $t_f$ (in.) | Senior & Gurney[1] | Design Curves Figure 2 | 3-D Finite Element | 3-D Finite Element | Experiment |
| .5 | 2.5 | 9.2 | 7.5 | 10.2 | 9.2 | 4.2 |
| 1 | 2.5 | 17.3 | 14.2 | 17.3 | 15.1 | 15.0 |
| .5 | 1.5 | 26.3 | 21.7 | 22.5 | --- | --- |
| .5 | 1 | 41.3 | 34.2 | 34.6 | 31.5 | 41.7 |
| 1 | 1.5 | 44.8 | 35.9 | 35.8 | --- | --- |
| 1 | 1 | 65.3 | 54.2 | 51.6 | 45.1 | 42.5 |

[a]All geometries included stiffeners spaced at 72 in, $b_f$ = 20 in., and b = 72 in.

finite element to Figure 6 results, between test and analytical results. Again, the agreement is very good for the comparisons.

## 7. Observations and Recommendations

Numerous conclusions and recommendations were previously noted in the summaries of each task report. In terms of overall observations and recommendations for the fatigue resistant design of runway girders the following should also be considered.

### 7.1 Review of Cracking in Welded Details

The following discussion explains the various cracking problems which have occurred in crane runway girders due to wheel induced stresses. These explanations are based on reported observations of in-service cracking.

#### 7.1.1 Cracking at Web-to-Flange Junction

The majority of in-service crane runway girders have partial penetration web-to-flange welds. The cracking occurring most frequently in these girders in midpanel locations is that initiating at the internal discontinuity of the weld. This cracking can be attributed to the three effects outlined below.

1. Initial Flaw – The internal discontinuity creates a sharp stress riser wherever incomplete bearing between the web and flange plates exist. This allows rapid initiation of cracks internal to the girder. Further, the rolling nature of the wheel load acts as a very efficient flaw finder. This leads to a series of cracks internal to the girder which coallesce and propagate outward toward the exposed surfaces. This behavior is evidenced by fractographic examinations showing coallescence, and by field observations of rapid surface crack growth along the length of welds.
2. Residual Stresses – In the welding process, the web and flange plates are butted against each other. The fit between these plates

is irregular. This leads to regions along the length where welding shrinkage acts to draw the plates closer creating a residual tension in the web plate. These stresses, superimposed on the applied compressive stresses, will create the possibility of fatigue cracking through the web thickness and along the girder until the residual tension is released. This explanation is reinforced by the existence of many cracks spaced randomly along existing girders. Further, observed crack openings in the unloaded state imply that high residual stresses have been released.

3. Irregular Rail/Flange Contact – It has been shown that very high weld stresses can exist due to irregularities in the contact zone between the rail and flange. This would explain why in-service cracking has been observed in a matter of months for 50-year design lives.

Other cracking occurring in the web-to-flange weld can occur at web toe defects. The initiation of this cracking can be attributed to severe undercut. The crack propagation is due to residual stresses at the toe and to both vertical and torsional loadings.

### 7.1.2 Cracking in the Stiffener Cope Region

It has been shown that when stiffeners allow top flange rotation, a severe web bending occurs within the region between the web-to-flange weld and the termination of the vertical stiffener-to-web weld. These stresses can result in cracking at the toe of each of these welds. The cracking at the web-to-flange weld propagates longitudinally toward the centerpanel region where the web bending is not as great. The cracking at the web-to-stiffener weld propagates into the web plate in a frowning shape. Both of these cracking problems are minimized by the use of a deep cope which reduces

the web bending stress. A more effective step is to weld the stiffener to the top flange ensuring that the cross section at the stiffener experiences little distortion.

### 7.1.3 Cracking in the Stiffener-to-Flange Weld

Cracking in the stiffener-to-flange welds occurs under the tensile stresses due to torsional loading. These cracks can propagate across one side of the girder until complete separation of a stiffener occurs. A girder with a completely cracked stiffener-to-flange weld can lead to web stress concentrations as in fitted stiffener details.

## 7.2 Review of Current Design Practice in the United States

The current recommendations in AISE TR No. 13 are aimed at combating the fatigue problems experienced in service. These measures can now be reviewed in light of the current work.

1. Full penetration web-to-flange welds and ultrasonic inspection have been recommended to eliminate cracks initiating internal to the weld. The problem of cracks initiating at the weld toe can be controlled by careful attention to weld toe profiles and elimination of undercut by grinding and/or peening.
2. Stiffener/flange welds have been recommended to allow stiffeners to reduce web stresses due to top flange rotation, and the web stress concentration effects in the region around the vertical termination of the stiffener. The current study has shown that these welds absorb significant vertical tensile stresses under torsional loadings and should be appropriately designed against fatigue. The weld detail recommended by AISE TR No. 13 for this detail is a full penetration weld. While partial penetration welds have been used in practice, the tensile stresses that occur due to torsional forces will

cause rapid propagation of an internal discontinuity. Thus, a full penetration weld is a necessary choice for this detail. However, appropriate design of the stiffener and selection of weld quality should be performed, based on the service load stresses.

3. The use of elastomeric rail pads, mentioned but not specifically recommended currently, should receive more consideration. This might be especially relevant as a life-prolongation measure for girders with partial penetration welds. (See Example Problem #3 below.)

## 7.3 Stress Analysis for Design

The web-to-flange welds of crane runway girders experience stress due to two types of loading: vertical loading and torsional loading. In this study, the relevant geometrical parameters for weld stresses due to each type of loading were determined. For vertical loading these are t, $t_f$, $b_f$, and d. For torsional loading the relevant parameters are $t_f$, a, t, b, $b_f$, and K. Experimental investigations showed that the rail/flange contact condition also has a strong influence on weld stresses. Design equations and charts for prediction of the stresses transmitted to the web-to-flange weld, Equations 2 and 3 and Figures 6 and 7, have been developed and scrutinized for extreme cases of contact conditions through extensive computer simulation and physical testing efforts. The example problems to follow illustrate how these analysis tools should be used in conjunction with fatigue resistance data.

## 7.4 Fatigue Resistance of Welded Details

The issue of fatigue resistance of the details recommended by the AISE is still open. Several foreign recommendations regarding this issue were discovered and reviewed. These are shown in Figures 8 and 9 and,

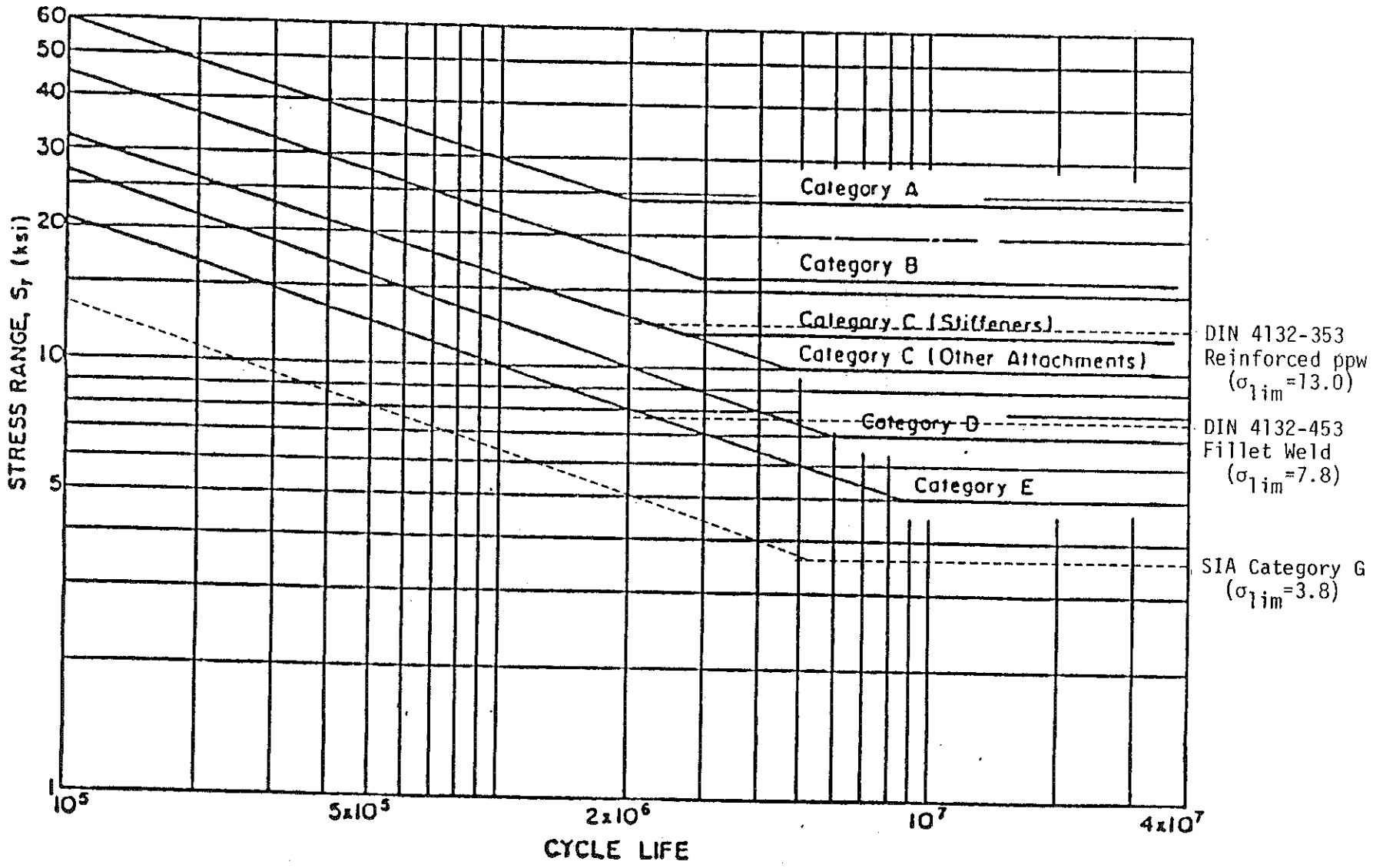


Fig. 8 S-N Curves for Partial Penetration Flange-to-Web Welds From Task III, Report #2.

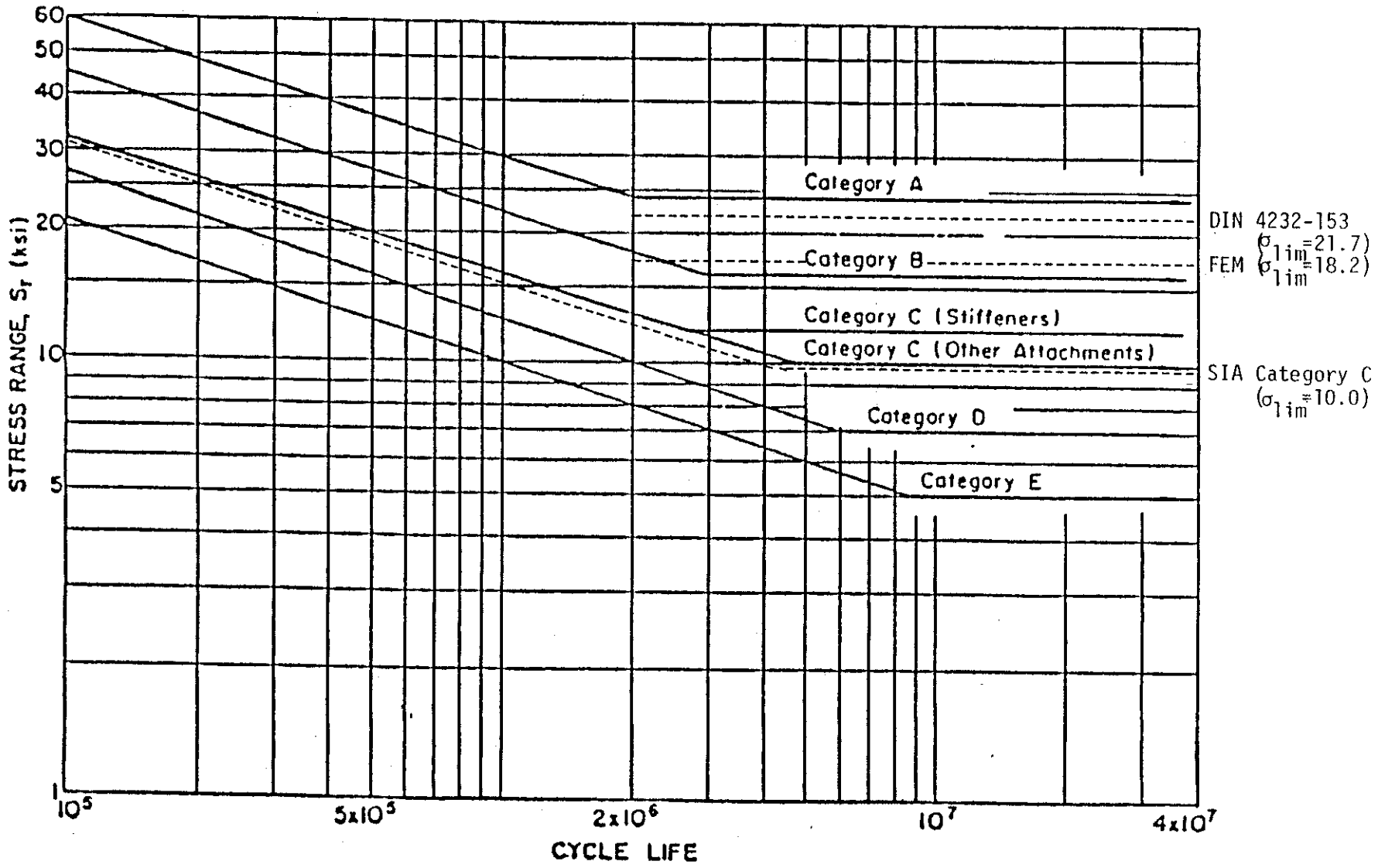


Fig. 9 S-N Curves for Full Penetration Flange-to-Web Welds From Task III, Report #2.

in conjunction with the improved analysis equations and charts developed in this project, can provide the designer with a more comprehensive technique for fatigue design than is currently available. However, much uncertainty exists in the accuracy and applicability of these European standards.

## 8. Example Problems

The following example problems indicate how the design recommendations for the web-to-flange weld could be used. Note that the following assumptions are in effect for all three example problems:

1. The design will be fatigue rated according to the S-N approach. Allowable stress range will be obtained from existing European standards as displayed in Figures 8 and 9.
2. The stress range will be computed as the sum of the vertical normal stress, $\sigma_{yy_{vert}}$, due to an applied vertical wheel load, P, and the additional vertical normal stress due to bending of the top of the web, $\sigma_{yy_{bend}}$, caused by an applied moment, M.
3. This moment will be caused by the vertical wheel load acting through the rail eccentricity which is 0.75t.
4. Additional moment due to lateral wheel load or other causes is not considered.
5. Unless otherwise noted, a uniform contact is assumed to exist between the rail and the flange.
6. Unless otherwise noted, vertical stiffeners are assumed to be welded to the bottom of the top flange.

Example Problem #1

Check design for infinite fatigue life:

$P = 62^k$

$t = 0.5$ in.

$t_f = 1.5$ in.

$b_f = 18$ in.

$d = 5.75$ in.

$\alpha = 0.33$ (from Figure 7)

$e = 0.75t = 0.375$ in.

$a = 60$ in.

From Equation 2,

$$\sigma_{yy_{vert}} = \frac{(53.73)(0.354)}{\sqrt{1 + 3.99(.125)(14.69)}}$$

$$\sigma_{yy_{vert}} = 6.55 \text{ ksi}$$

Use Figure 6,

Get $M = 62^k \times 0.375 = 23.25$ in-k

Get $K = K_f + K_r$

$= 20.25 \text{ in}^4 + 9.07 \text{ in}^4$

$K = 29.32 \text{ in}^4$

Get $D = \frac{Et^3}{12(1 - \mu^2)} = 325.8$ k-in

Get $\frac{GK}{Da} = \frac{(11.5 \times 10^3 \text{ ksi})(29.32 \text{ in}^4)}{325.8 \text{ k-in} \times 60 \text{ in}}$

$= 17.25$

Check for q = 4d

Get $q = 5 \times 5.75$ in $= 28.75$ in

23 in

Get $\frac{q}{a} = \frac{28.75 \text{ in}}{60 \text{ in}} = 0.48$ 0.38

$\frac{m_{yy_{max}}}{M}^{q} = 0.032$ 0.030

Get $m_{yy_{max}} = \frac{(0.032)(23.25)}{28.75}$

$= 0.026$ in-k/in 0.030 in-k/in

Get $\sigma_{yy_{bend}} = \frac{m_{yy_{max}}}{S} = \frac{0.026 \times 6}{(0.5)^2}$

$= 0.62$ ksi

Get Total $\sigma_{yy} = 6.55 + 0.62 = 7.2$ ksi

Check allowable stress range:

Case 1: Partial Penetration Weld, Figure 8

a. SIA Category G

$\sigma_{yy_{max}} > \sigma_{lim}$

Expected life $\approx 7 \times 10^5$ wheel passages

b. DIN 4132-453 Fillet Weld

$\sigma_{yy_{max}} < \sigma_{lim}$

c. DIN 4132-353 Reinforced PPW

$\sigma_{yy_{max}} < \sigma_{lim}$

Case 2: Full Penetration Weld, Figure 9

$\sigma_{yy_{max}} < \sigma_{lim}$

For SIA, FEM, and DIN category curves.

Example Problem #2

Check design for infinite fatigue life:

$P = 200^k$

$t = 1$ in.

$t_f = 2$ in.

$b_f = 20$ in.

$d = 6$ in. (175# rail)

$\alpha = 0.5$ (from Figure 7)

$e = 0.75t = 0.75$ in.

$a = 60$ in.

From Equation 2,

$$\sigma_{yy_{vert}} = \frac{(65)(0.42)}{\sqrt{1 + 2.66(0.175)(9)}}$$

$$\sigma_{yy_{vert}} = 12 \text{ ksi}$$

Use Figure 6,

Get $M = 200^k \times 0.75$ in $= 150$ in-k

Get $K = K_f + K_r = \frac{1}{3} b_f (t_f)^3 + K_r$

$K_r \cong 20$ in$^4$ (See Torsion in Structures, Kollbrunner and Basler, Springer Verlag, 1969, pp. 267-272.)

$K = 53.3 + 20 = 73.3$ in$^4$

Get $D = 2606$ in-k

Get $\frac{GK}{Da} = \frac{(11.5 \times 10^3 \text{ ksi})(73.3 \text{ in}^4)}{(2606 \text{ in-k})(60 \text{ in})}$

$= 5.4$

Get $q = 5 \times 6$ in $= 30$ in

Get $\frac{q}{a} = \frac{30 \text{ in}}{60 \text{ in}} = 0.5$

$$\frac{m_{yy_{max}}}{M} = \frac{q}{0.10}$$

$$m_{yy_{max}} = \frac{(0.10)(150\ \text{k-in})}{30\ \text{in}} = 0.5\ \frac{\text{in-k}}{\text{in}}$$

$$\sigma_{yy_{bend}} = \frac{(0.5\ \text{in-k/in})(6)}{1^3} = 3\ \text{ksi}$$

Get total $\sigma_{yy} = \sigma_{yy_{vert}} + \sigma_{yy_{bend}} = 15$ ksi

Check allowable stress range:

Case 1: Partial Penetration Weld, Figure 8

a. SIA Category G,

$$\sigma_{yy_{max}} \gg \sigma_{lim}$$

Expected life $< 1 \times 10^5$ wheel passages

b. DIN 4231-452, Fillet Weld

$$\sigma_{yy_{max}} > \sigma_{min}$$

Expected life $\approx 2 \times 10^5$ wheel passages

c. DIN 4232-353 Reinforced PPW

$$\sigma_{yy_{max}} > \sigma_{lim}$$

Expected life $\approx 1 \times 10^6$ wheel passages

Case 2: Full Penetration Weld, Figure 9

a. SIA Category C

$$\sigma_{yy_{max}} > \sigma_{lim}$$

Expected life $\approx 1 \times 10^6$ wheel passages

b. For FEM and DIN

$$\sigma_{yy_{max}} > \sigma_{lim}$$

Example Problem #3

Check design for infinite fatigue life. All design parameters the same as in Problem #1. However, point contact between the rail and the flange is assumed.

Case 1: No Rail Pad

From Equation 3,

$$\sigma'_{yy_{vert}} = \frac{0.65P}{tt_F}\left[\frac{b_F}{t}\right]^{-.29}$$

$$\sigma'_{yy_{vert}} = 19 \text{ ksi}$$

Using Figure 6,

$$\sigma'_{yy_{bend}} = 0.6 \text{ ksi}$$

Get total $\sigma'_{yy} = 19 \text{ ksi} + 0.6 \text{ ksi} = 19.6 \text{ ksi}$

Check Allowable Stress Range:

$\sigma'_{yy}$ exceeds the fatigue limit for all category curves except the DIN 4232-153 for which the limit is 21.7 ksi.

Case 2: Use Rail Pad

Assume a 35% reduction in $\sigma'_{yy_{vert}}$ due to pad:

$$\sigma_{yy} = 0.65 \times 19.6 = 12.75 \text{ ksi}$$

Check Allowable Stress Range:

The design is now adequate for a full penetration detail under DIN 4232-153 and FEM standards, and for a reinforced partial penetration weld under the DIN 4132-353 standard.

Example Problem #4

Re-perform Example Problem #2 but without intermediate stiffeners, or with intermediate stiffeners not welded to the top flange. For this case a = girder span. Assume a span of 600 in.

$$\sigma_{yy_{vert}} = 11.96 \text{ ksi} \quad \text{(unchanged)}$$

Now use Figure 6b (see notes below),

$$\frac{GK}{Da} = 0.54$$

$$\frac{q}{a} = 0.05$$

$$\frac{m_{yy_{max}}}{M}\,q = 0.22$$

$$m_{yy_{max}} = 1.15 \frac{\text{in-k}}{\text{in}}$$

$$\sigma_{yy_{bend}} = 6.9 \text{ ksi}$$

Get total $\sigma_{yy} = \sigma_{yy_{vert}} + \sigma_{yy_{bend}} = 18.9$ ksi

Check Allowable Stress Range:

This design is inadequate with either a full or a partial penetration weld under all standards shown in Figures 8 and 9, except the DIN 4232-153 (see note below).

**Note:** When using Figure 6b, the number of cylces of load per crane passage is not equal to the number of wheels, as is the case for Figure 6a. When vertical stiffeners are not available for or capable of resisting flange torsion, there is substantial overlap of the moment distributions from successive wheel loads. Hence, one full stress range occurs for each crane passage. This phenomenon reduces substantially the

number of cycles experienced by each in the weld detail. However, it also means that the stress range, $\sigma_{yy_{bend}}$, computed from Figure 6b, is a lower-bound. This is because it is the peak value for an individual wheel. A more accurate calculation would require information on wheel spacing and the use of the complete solution, not just the peak value, for the moment transmitted to the web from a single wheel load. See Task III, Report #2, pp. 183-185, for additional information.